Orbital
The electronic journal of chemistry

the electronic journal of chemistry

Full Paper | http://dx.doi.org/10.17807/orbital.v17i5.23217

DFT and Molecular Docking Studies on Antimicrobial Active Synthetic Derivatives of Benzimidazo-quinazoline

Gopal Krishna Murthy HR*[a], Revanasidappa HD[a], Avinash KO[b], Vasanth Kumar BC[c], Prema M[a], and Keshav Kumar Harish[e]

The development of new antibiotics is crucial due to the growing global threat posed by microbial diseases and the resulting increase in medication resistance. A nitrogen-containing heterocycle with a variety of pharmacological actions, including antibacterial and anticancer effects, is benzimidazole. This study explores the antimicrobial potential of synthesized compounds of Benzimidazo-quinazoline motifs' subjecting them to molecular docking studies against Dihydroorotase from *E. Coli* and Thymidylate kinase from *Staphylococcus aureus*. Compounds L2 and L3 showed strong affinities for Dihydroorotase and Thymidylate kinase, respectively, according to molecular docking, which revealed potential interactions. Although more research on other microbial targets is necessary, the study highlights the potential of benzimidazole-quinazoline in blocking bacterial proteins. DFT calculations suggested that L2 and L3 compounds showed the lowest gap energy and were chemically reactive, and promise to serve as potential anti-microbial drug. In general, this study represents a noteworthy advancement towards the creation of potent antimicrobial drugs.

Graphical abstract

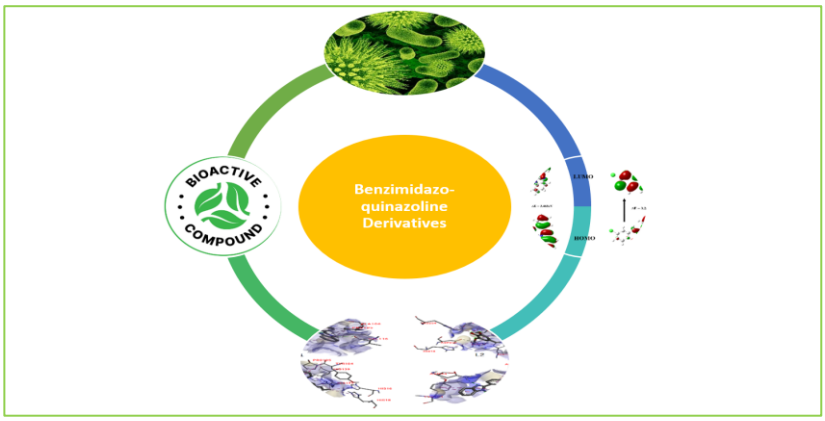

Keywords

Antimicrobial
Gram-positive
Gram-negative
Synthetic compounds

Article history

Received 10 Jun 2025
Revised 25 Jul 2025
Accepted 25 Jul 2025
Available online 18 Dec 2025

Handling Editor: Marcos S. Amaral

1. Introduction

In recent times, the rise in the incidence and fatality of microbial infections poses a significant global challenge [1]. The escalating prevalence of drug resistance, encompassing multiple drug resistance (MDR) and extensive drug resistance

[a]Department of Chemistry, University of Mysore, Manasagangothri, Mysuru, Karnataka, India. [b]Biochemistry Department of Life Sciences, Acharya Bangalore B School, Bangalore,Karnataka, India. [c] Department of Chemistry, DRM College, Davanagere, Karnataka, India. [d]Department of Chemistry, GFGC, Yelahanka, Bangalore, Karnataka, India. [e]Department of Physics, University of Mysore, Manasagangotri, Mysuru, Karnataka. *Corresponding author: **gkmurthy123@gmail.com**

(XDR) among infectious bacterial pathogens [2] has substantial implications for the management of infectious diseases, potentially heightening the threat of widespread illness [3]. Consequently, there is an imperative need to innovate and create novel classes of antibiotics [4]. Nitrogen-containing heterocycles, like benzimidazole, are important biological and pharmacological substances with a variety of functions ranging from antibacterial to anticancer [5]. The active pharmacophore of albendazole, mebendazole, and thiabendazole is benzimidazole, which is a crucial component of these commonly used anthelmintic medicines [6]. Interestingly, a key component of vitamin B12 is the benzimidazole derivative 5,6-dimethyl-1-(α-D-ribofuranosyl)benzimidazole [7]. The antibacterial efficacy, antiviral qualities, anticancer activity, antiprotozoal effects, analgesic potential, anti-inflammatory traits, antipyretic activity, and antiangiogenics features of a wide range of benzimidazole derivatives have all been studied [8]. Quinazoline and related compounds are strong cytotoxic agents that have exhibited noteworthy biological activity [9]. The anticancer, fungicidal, anti-inflammatory, anti-hypertensive, and analgesic actions of substituted quinazolines have been demonstrated. It has been demonstrated that the biological activity of quinazolines is increased when benzimidazoles and quinazolines fuse to create Benzimidazo-quinazoline motifs [10]. Recognizing these facts and continuation of our previous work hybrid molecules incorporating benzimidazoles and quinazolines were designed and synthesized.

The benzimidazo-quinazoline derivatives (L1–L4) differ structurally from classical benzimidazole drugs like albendazole and mebendazole. While the latter possess a benzimidazole core with a 2-position methyl carbamate essential for β-tubulin inhibition and antiparasitic activity [11], L1–L4 feature a rigid, fused tricyclic benzimidazo-quinazoline system with extended conjugation, enhancing their interaction with diverse biological targets. Specific substitutions further influence their bioactivity: L1 has a methoxy-phenol group offering hydrogen bonding potential; L2 includes dimethoxy groups to improve lipophilicity; L3 bears a chloro-phenol moiety contributing to electronic modulation and metabolic stability. L4 contains a 4-bromo and 6-methoxy-phenol substitution, where the bromine acts as a bulky, electron-withdrawing group, potentially enhancing binding affinity through halogen bonding and improving metabolic stability, while the methoxy-phenol moiety supports hydrogen bonding and antioxidant activity. These structural enhancements suggest improved pharmacokinetics and broader antimicrobial or anticancer potential compared to traditional benzimidazoles [11, 12].

We subjected our target compounds to molecular docking studies on different target protein to explore mode of action. The two proteins that we looked into in this work are Thymidylate kinase (TMK) from *S. aureus* and Dihydroorotase from *E. coli.* These proteins are important targets in the search for new antimicrobial drugs. The reversible conversion of N-carbamyl-1-aspartate to dihydro-L-orotate is catalysed by the enzyme dihydroorotase, which is essential for the production of pyrimidines [13]. Predominantly found in bacteria and fungi, Dihydroorotase inhibitors exhibit promise as antimicrobial agents, making them subjects of significant interest in drug discovery efforts [14]. On the other hand, because Thymidylate Kinase (TMK) is essential to the production of bacterial DNA, it is a desirable target for treatment in the fight against bacterial infections. TMK inhibitors present a strong opportunity for the development of novel antibacterial medicines with increased potency and selectivity because of their crucial role in DNA replication [15]. Our work intends to investigate the capacity of synthesized compounds to interact with anti-microbial target protein through the use of molecular docking and advanced computational approaches. At the same time we explored antibacterial activity of the compounds against two commonly affected bacterial species i.e *E. coli* and *S. aureus* through invitro studies (Disc diffusion assay). Our objective for carrying out this research is to find possible inhibitors that could work as an antibacterial drug.

2. Material and Methods

2.1 In-silico study

2.1.1 Protein selection

With a comprehensive review of the literature, we were able to identify proteins from both gram-positive and gram-negative species. Thymidylate kinase from *Staphylococcus aureus* (4QGG) [16] and dihydroorotase from *E. Coli* (2EG7) [17] were the chosen proteins. As shown by the results of earlier investigations, these specific proteins were selected because of their known antibacterial properties.

2.1.2 Ligand preparation

Ligands was selected from vasantha kumar B.C, thesis 2018 [18]. Four ligands were selected with the following details were drawn using chemsketch and converted PDB for further docking.

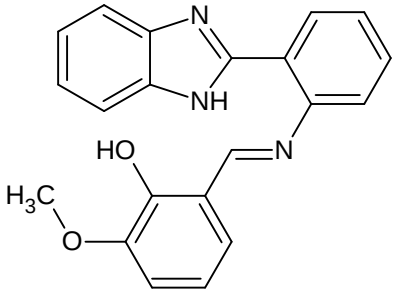

L1. 2-(5,6-dihydro-benzo[4,5]imidazo[1,2-c]quinazolin-6-yl)-6-methoxy-phenol.

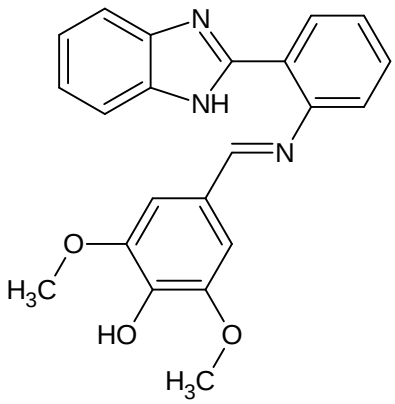

L2. 4-(5,6-dihydro-benzo[4,5]imidazo[1,2-c]quinazolin-6-yl)2,6-dimethoxy-phenol.

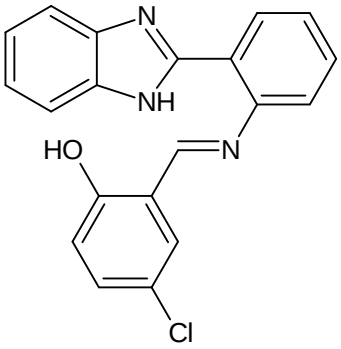

L3. 4-chloro-2-(5,6-dihydro-benzo[4,5]imidazo[1,2-c]quinazolin-6-yl)-phenol.

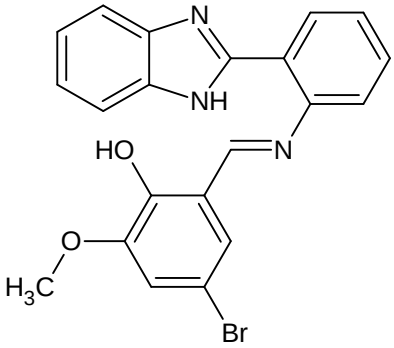

L4. 4-bromo-2-(5,6-dihydro-benzo[4,5]imidazo[1,2-c]quinazolin-6-yl)-6-methoxy-phenol.

2.1.3 Protein retrieval

The three-dimensional structure of the Thymidylate kinase from *Staphylococcus aureus* (4QGG) and dihydroorotase from *E. Coli* (2EG7) was obtained from the Protein Data Bank (PDB). Pymol software was used to remove or modify any non-standard amino acids present in the initial structure.

2.1.4 Binding Site Prediction

The potential binding sites of the protein were predicted using the *in-silico* tool CASTp (**http://sts.bioe.uic.edu/castp/index.html?3trg)** on the refined structure obtained.

2.1.5 Protein Structure Validation

The Thymidylate kinase from *Staphylococcus aureus* (4QGG) and dihydroorotase from *E. Coli* (2EG7) structure were validated using the Ramachandran plot generated by the PROCHECK RAMPAGE option in UCLA-DOE LAB- SAVES v6.0 (**https://saves.mbi.ucla.edu/**). The results indicate a stable and well-validated structure.

2.1.6 Molecular Docking Analysis

Molecular Docking was carried out between synthetic compounds and selected proteins using Autodock Vina. The proteins and the ligands both were in PDBQT format, and the active site residues were marked to define the grid box using Autodock tools software. The highest orientation with the lowest binding affinity (Kcal/mol) values was obtained.

2.1.7 Molecular Docking Visualization

The docked conformation of the ligands against the proteins was visualized using BIOVIA Discovery Studio Visualizer. This program was used to create 3D and 2D visualizations of the interactions between protein and ligands, including hydrogen bonds, hydrophobic interactions and bond length.

2.1.8 Density Functional Theory (DFT) Calculations

Gaussian et.al [19] was used to carry out DFT studies for the lead compounds L2 and L3 respectively. The molecular structures of both the ligands were created and examined with GaussView 5. The geometries were optimized at the B3LYP level with a 6-311++G (d, p) basis set. [20].

2.2 Invitro study

2.2.1 Antimicrobial assay (disc diffusion assay)

Using the disc diffusion technique, the antibacterial activity of the L1, L2, L3 and L4 compounds was assessed. One gram-positive bacteria, Staphylococcus aureus and one gram-negative bacteria, *Escherichia coli* were used in the test microorganisms. All of the isolated bacteria were purchased from ATCC, and the cultures were then subcultured in Luria Broth (LB-HiMedia) for roughly twenty-four hours. Spread on nutrient agar plates, the bacterial concentration was adjusted to 1.5×10^8 CFU/ml using the 0.5 McFarland Standard. The antimicrobial activity against *Staphylococcus aureus* and *Escherichia coli* was assessed using varying concentrations of compounds dissolved in 0.5% DMSO, ranging from 100 µg/ml, 75 µg/ml, 50 µg/ml, and 25 µg/ml. The results were compared to the standard medication tetracycline, which was used as a control. Additionally, the bacterial culture plates were incubated for approximately twenty-four hours at 37℃. Following incubation, measurements were made of the zone of inhibition surrounding the disk of each compound tested [21].

3. Results and Discussion

This study aimed to test the antimicrobial activity of some newly synthesized Benzimidazo-quinazoline motifs and to identify the possible underlying their interaction with gram-positive and gram-negative microbes protein. With the use of cutting-edge bioinformatics tools and software, the study performed an extensive *insilico* evaluation of four synthesized compounds against the Dihydroorotase from *E. coli* and Thymidylate kinase from *Staphylococcus aureus*. Similar studies involving benzimidazole derivatives, anti-microbial and anti-malarial activities along with DFT [21-26].

3.1 In silico study

3.1.1 Protein selection

Dihydroorotase (DHOase) is a vital enzyme in the de novo pyrimidine biosynthesis pathway of *Escherichia coli*, catalyzing the reversible conversion of carbamoyl aspartate to dihydroorotate. This step is essential for DNA and RNA synthesis. DHOase typically exists as a homodimer with an α/β fold, and its catalytic mechanism involves a key histidine residue that initiates nucleophilic attack. Structural and functional insights from X-ray crystallography, molecular dynamics, and kinetic studies have defined optimal conditions for activity. Moreover, computational docking has identified potential inhibitors, highlighting DHOase as a promising antimicrobial drug target [27- 29].

Thymidine kinase (TK) is a key enzyme in the pyrimidine salvage pathway, catalyzing the ATP-dependent phosphorylation of thymidine to dTMP—an essential step in DNA synthesis and repair. In *Staphylococcus aureus*, TK displays a unique conformation facilitating effective binding of ATP and thymidine, with critical residues mediating substrate recognition. Structural studies show that TK activity is highly pH-dependent, with optimal function at physiological pH and significant structural disruption at acidic conditions. Recent research has identified potential TK inhibitors that exploit its structural features to enhance binding, offering a promising strategy against antibiotic-resistant *S. aureus* strains (30, 31).

3.1.2 Protein Structure Validation

The structures of both proteins were validated using the Ramachandran plot (Figure 1) generated by PROCHECK RAMPAGE. The results showed in Table 1, that the residues were located in the favorable regions, and allowed region indicating that the structure was suitable for further molecular docking studies.

Table 1. Ramachandran plot favourable regions of Dihydroorotase and Thymidylate kinase proteins.

Sl No	Protein Structure	Number of Residues in Favoured Regions (%)	Number of Residues in Allowed Regions (%)	Number of Residues in Disallowed Regions (%)
1	Dihydroorotase (2EG7)	88.1	11.2	0.0
2	Thymidylate kinase (4QGG)	92.4	7.1	0.6

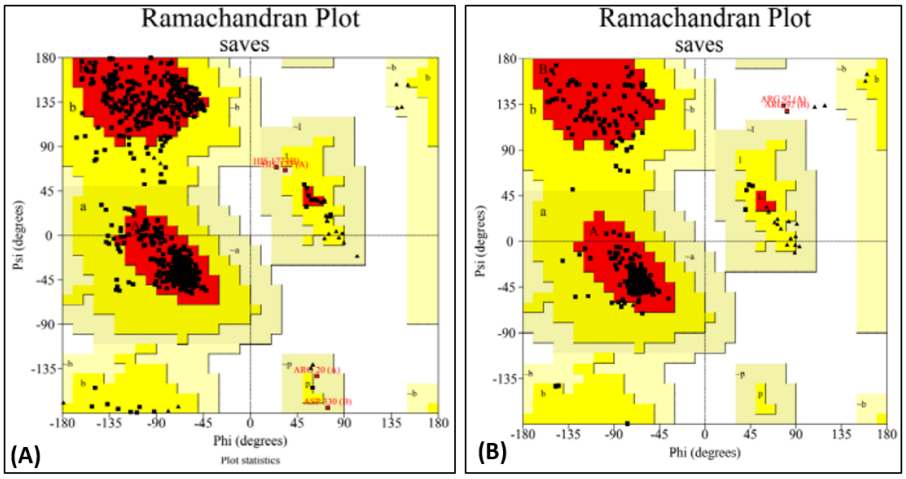

Fig. 1. The Ramachandran plot generated from RAMPAGE. The Ramachandran plot representing energetically allowable regions for backbone dihedral angles ψ vs. φ amino acid residues in selected protein structure. (A) Dihydroorotase from *E. coli* (B) Thymidylate kinase from *Staphylococcus auerus*.

3.1.3 Protein-Ligand Interaction

The molecular docking studies between the selected protein and the synthetic compounds revealed key interactions between the ligands and the protein. The results, as presented in Figure 2, showed that L2 had the highest binding score, indicating a strong binding affinity for the Dihydroorotase *E. coli* protein and as for the Thymidylate kinase, L3 had the highest binding score, indicating a strong binding affinity.

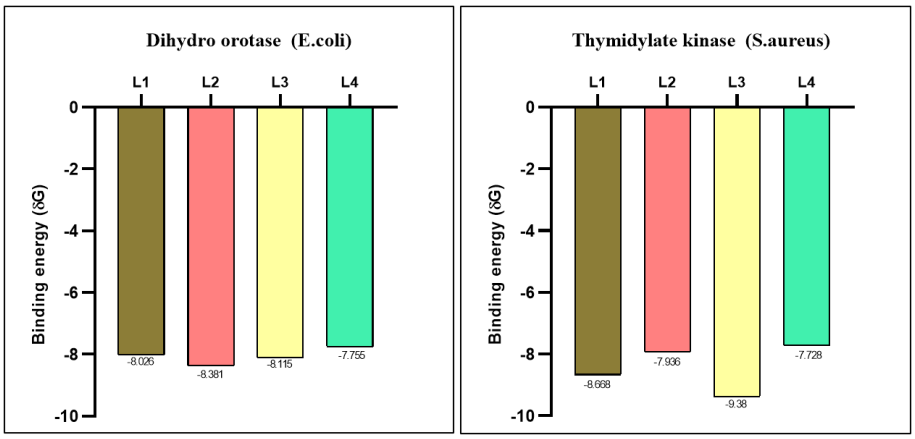

Fig. 2. Barplot of Molecular Docking results between selected proteins against S -*9/8+*8ynthetic compounds (the binding energy value δG is shown in minus kcal/mol).

3.1.4 Analysis of selected protein and synthetic compound interactions

The results of the molecular docking studies between the selected protein and the synthetic compounds are presented in Figures 3 and 4. The best-docked pose among the various compounds was selected based on the lowest binding affinity (Kcal/mol) values. The interactions between the selected ligands and the protein were analysed using the BIOVIA Discovery Studio Visualizer software, highlighting the key binding residues. The studied ligands were observed to form hydrogen bonds with the protein that were shorter than 2.75 nm in length and were also partially surrounded by hydrophobic interactions. Data revealed that L2 and L4 formed several hydrogen bonds with key amino acid residues in the Dihydroorotase *E. coli* protein and the Thymidylate kinase from *Staphylococcus aureus* (Table 2).

As seen in the 3D structures (Figures 3 and 4), these hydrogen bonds probably play a part in the stable binding between the ligands and the proteins. They also likely contribute to the observed hydrophobic interactions. They also likely contribute to the observed hydrophobic interactions. Our study's findings indicate that the active benzimidazole-quinazoline molecule under investigation may be able to actively interact with Thymidylate kinase and dihydroorotase enzyme. It is imperative to acknowledge, yet, that a constraint on our findings is the lack of data concerning the possible influence on additional microbial targets, including DNA gyrase, dihydropteroate synthase, and dihydrofolate reductase. These targets have been shown in earlier research to be crucial for antimicrobial action [22–24].

Table 2. Number of hydrogen bonds between ligands and proteins.

Protein	Ligand	Number of Hydrogen Bonds	Number of Residues
Dihydroorotase	L1	1	VAL116
	L2	0	
	L3	0	
	L4	2	ASN44, ALA266
Thymidylate kinase	L1	1	GLU37
	L2	3	GLU37, GLN101
	L3	2	GLU37
	L4	1	GLN101

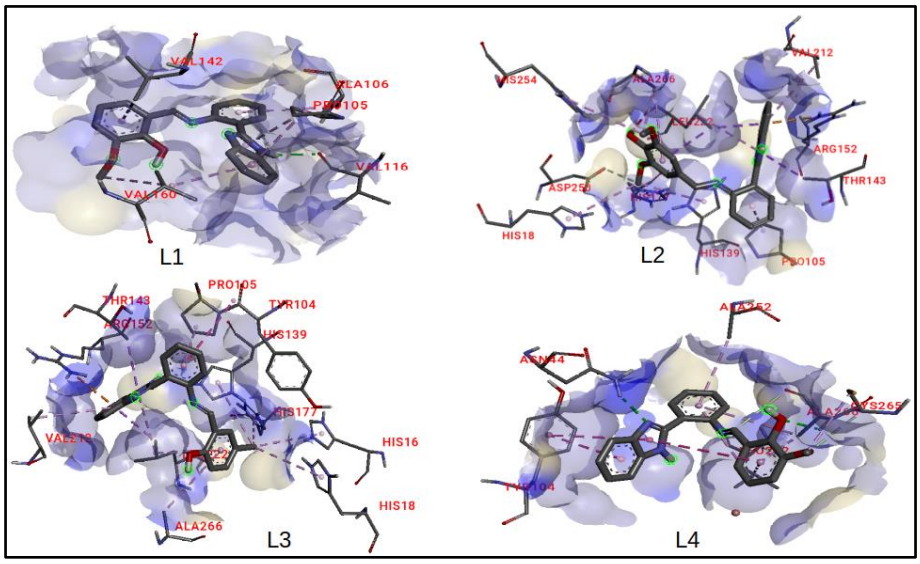

Fig. 3. 3D structures of synthetic compounds docked with Dihydroorotase.

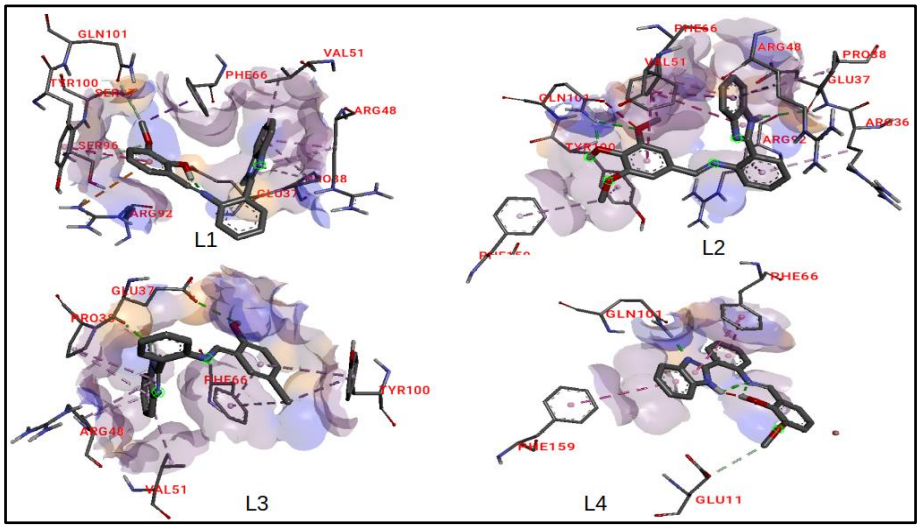

Fig. 4. 3D structures of synthetic compounds docked with Thymidylate kinase.

3.1.5 Density Functional Theory study

The kinetic stability and chemical reactivity of L2 and L3 were assessed using Frontier Molecular Orbital (FMO) analysis via DFT method with an appropriate basis set [32]. By examining the HOMO-LUMO energy gap levels, we can gain important insights into the biological mechanism [33, 34]. Accordingly, the highest occupied molecular orbitals (HOMO) signify electron donor capability, while the lowest unoccupied molecular orbitals (LUMO) indicate electron acceptor capacity [34] (Figure 6). The energy gap (Eg) provides a measure of the molecule's chemical reactivity and stability; a smaller gap means higher chemical reactivity and lower stability, while a larger gap indicates lower chemical reactivity and higher stability.

The MESP values for L2 and L3 are shown in Figure-5 using a colour gradient scale. The plot values range from negative to positive, with deep red indicating negative (electron-rich) areas and deep blue indicating positive (electron-deficient) areas. Figure 5 illustrates the highest occupied and lowest unoccupied molecular orbital densities of the ligands L2 and L3 respectively. The Table 3 lists the global chemical reactivity descriptors derived from the orbital energies. The global hardness is found to be 1.730 and 1.629 eV for L2 and L3, respectively.

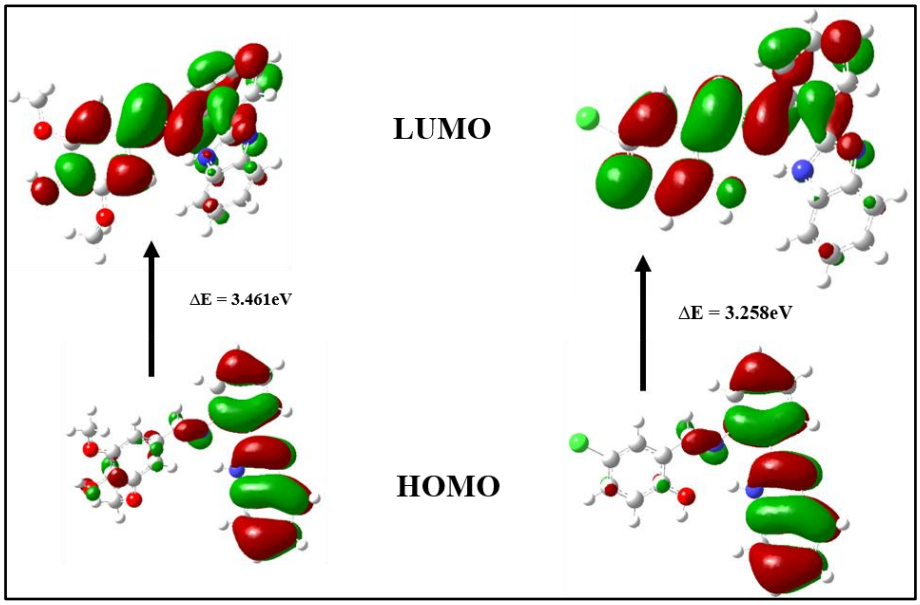

Fig. 5. Frontier molecular orbital (FMO) plots for L2 and L3.

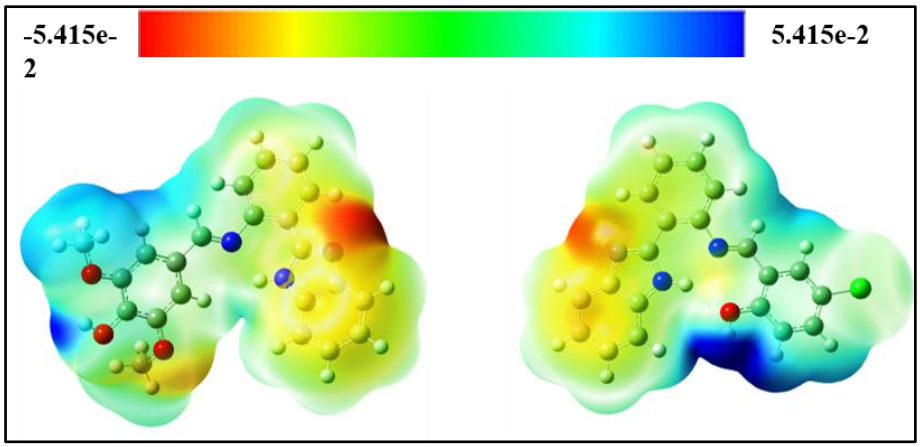

Fig. 6. Molecular electrostatic potential (MEP) map L2 and L3.

The L3 is quite stable with a chemical potential of -7.044 eV as compared to L2, indicating a high electron-accepting capability showing with a reasonable chemical potential, suggests strong electron acceptance, while a low potential indicates strong electron donation ability [27]. It is observed from the Figure 5 that the HOMOs are localized in the region of 5, 6-Dihydro-benzo [35, 36] imidazole [1,2-c] quinazolin-6-yl moieties in both the compounds, as the core structures remain the same. The LUMO is delocalized in 2, 6 dimethoxy phenol moiety in L2 and 4-chloro phenol moiety in L3, respectively. The three-dimensional molecular electrostatic potential (MESP) plot provides an in-depth view of a molecule's electronic structure by showing the distribution of electron density and polarization around the molecule. Regions with MESP values close to zero represent a balance in electron density or charge neutrality. It is observed from the Figure 6, that the nitrogen atom of imidazole group of both ligands is surrounded with red colour region. It acts as an electron-rich prone area [36]. Conversely, the dark blue area around the –OH group substituents are electron-deficient and tend to attract electron rich regions. The reactive sites found in both the compounds exhibit significant hydrogen bond interactions and demonstrate its importance towards biological activity at the respective active sites of the enzyme target.

Table 3. Global Chemical Reactivity Descriptors (GCRD) Parameters of L2 and L3.

GCRD Properties	Symbol / Formula	L2	L3
Energy	E (a. u.)	-1240.02	-1470.53
E_{HOMO}	E_H (eV)	-5.670	-5.782
E_{LOMO}	E_L(eV)	-2.209	-2.524
$\Delta E_{LUMO-HOMO}$	$E_g = E_{L-H}$ (eV)	3.461	3.258
Ionization potential(I)	$I = -E_H$(eV)	5.670	5.782
Electron affinity (A)	$A = -E_L$(eV)	2.209	2.524
Global Hardness (η)	$\eta = (E_{L-H})/2$ (eV)	1.730	1.629
Softness (S)	$S = 1/2\eta$(eV^{-1})	0.289	0.306
Chemical potential(μ)	$\mu = (E_H+E_L)/2$ (eV)	-6.774	-7.044
Electronegativity (χ)	$\chi = -\mu$ (eV)	6.774	7.044
Electrophilicity (Ψ)	$\Psi = \mu^2/2\eta$ (eV)	13.26	15.18

It is observed from the Table 3 that the computed HOMO values for L2 and L3 were found to be -5.670 eV and -5.782eV and the LUMO values with 2.209 and 2.524eV, respectively. The energy gap is found to be 3.461 eV (L2) and 3.258eV (L3) respectively, suggesting that there is a slight change in its values due to the effect of substituents attached in the aromatic rings of both molecules.

Future studies might consider concentrating on the effects of these goals. Considering the limitations, the results of this investigation call for more research. The most promising compounds (L2 and L4) would next be subjected to in vitro experiments to confirm their expected binding affinities and inhibitory effects on the target enzymes. Furthermore, to clarify the precise processes by which these substances block the enzymes, mechanistic investigations would be essential.

3.2 Invitro studies

3.2.1 Antimicrobial activity (Disc diffusion assay)

The antimicrobial potential of the synthesized benzimidazo-quinazoline derivatives was assessed using the agar disc diffusion method against selected Gram-positive (*Staphylococcus aureus*) and Gram-negative (*Escherichia coli*) bacterial strains. The results, summarized in Table 4 and Figure 7, are reported as the diameter of the zone of inhibition (mm). All four derivatives exhibited significant antibacterial activity, with varying but comparable inhibition zones against both bacterial species.

Table 4. antimicrobial activity zone of inhibition of all the four compounds against *E. coli* and *S. aureus*.

Extract	Concentration (μg/ml)	*L1* (mm)	*L2* (mm)	*L3* (mm)	L4 (mm)
E. coli	200	0.3	0.1	0.2	0.4
	400	0.7	0.3	0.4	1.3
	600	1.2	1.3	1.5	1.9
	800	2.7	2.6	2.6	3.2
	1000	4.4	3.5	3.7	4.1
S. aureus	200l	0.4	0.2	0.2	0
	400	0.5	0.2	0.4	0.2
	600l	1.7	1.3	1.2	1.9
	800	3.7	2.7	2.9	3.2
	1000	4.1	3.6	3.7	3.9

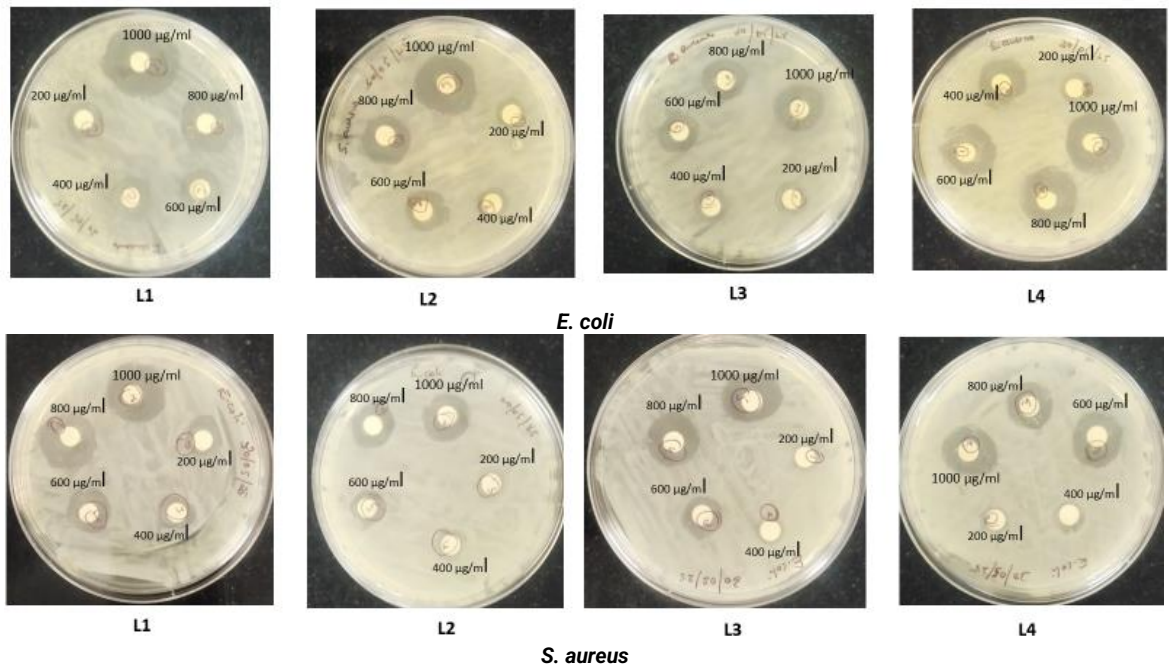

Fig. 7. Antimicrobial activity of all the four benzimidazo-quinazoline derivatives against *E. coli* and *S. aureus*.

The benzimidazo-quinazoline scaffold is known for its broad pharmacological profile, and its structural features—such as the fused heterocyclic system, electron-rich nitrogen atoms, and substituent variability—are believed to contribute to its antimicrobial activity. These compounds may exert their effects by interacting with bacterial DNA, inhibiting key enzymes, or disrupting membrane integrity, as suggested by previous studies on similar heterocycles [37, 38].

Importantly, all four compounds showed consistent inhibitory effects against *S. aureus and E. coli,* indicating that the derivatives can act against both Gram-positive and Gram-negative bacteria. This broad-spectrum activity is noteworthy,

considering the structural and permeability differences in the cell walls of these bacterial groups. While the disc diffusion assay provides a preliminary assessment, further quantitative studies—such as minimum inhibitory concentration (MIC) and time-kill assays—are needed to validate and detail the antimicrobial potential. Moreover, structure-activity relationship (SAR) studies could help identify the functional groups responsible for the observed activity.

4. Conclusions

This work investigated the possible inhibitory effects of synthetic substances on Thymidylate kinase and Dihydroorotase using *in-silico* approaches. The findings showed that the compounds selected (L1 to L4) and the target proteins interacted well, with L2 and L3 showing the highest binding affinities for Thymidylate kinase and Dihydroorotase, respectively. These substances establish important hydrogen bonds with the enzymes, which may indicate possible inhibitory mechanisms. Though the *in-silico* techniques yielded significant insights, additional wet laboratory tests are required to confirm the anticipated binding affinities and inhibitory effects. To validate the preliminary results and evaluate the functional effect of these drugs on the target enzymes, in vitro experiments will be essential. Furthermore, mechanistic investigations will be necessary to clarify the precise mechanisms by which these substances block the enzymes. Ultimately, in vivo investigations will be necessary to assess these potential candidates' safety and effectiveness in a whole-organism environment. These compounds show promise for further development as possible treatments targeting Thymidylate kinase and Dihydroorotase provided that the in vitro and in vivo studies validate the preliminary findings. DFT calculations suggested that studied compounds showed the lowest gap energy and chemically reactive. The results obtained from molecular docking and DFT calculation are in good agreement suggesting the potential use of the synthesised compounds as anti-microbial potency. The in vitro antimicrobial studies demonstrated inhibitory effects consistent with the in silico predictions, confirming the reliability of molecular docking and computational analysis in forecasting biological activity. This correlation supports the potential of the synthesized benzimidazo-quinazoline derivatives as promising antimicrobial agents and validates the use of in silico approaches for early-stage drug screening.

Acknowledgments

The corresponding author like to thank to the Department of Collegiate Education, Karnataka, India and the University of Mysore. The author Keshav Kumar Harish would like to acknowledge DST-KSTePS, Government of Karnataka for providing financial assistance.

Author Contributions

GKMHR and RHD: Literature Survey, Data collection, Data analysis, Data validation. AKO: Biological activity. VKBC: Synthesis. SC: Molecular docking study. KKH: DFT study.

.

References

[1] Aydın, M.; Azak, E.; Bilgin, H.; Menekse, S.; Asan, A.; Mert, H. T. E. *Eur. J. Clin. Microbiol. Infect. Dis.* **2021**, *40*, 1737. [Crossref]

[2] Mirzaei, B.; Bazgir, Z. N.; Goli, H. R.; Iranpour, F.; Mohammadi, F.; Babaei, R. *BMC Res. Notes* **2020,** *13*, 380. [Crossref]

[3] Cantas, L.; Shah, S. Q. A.; Cavaco, L. M.; Manaia, C. M.; Walsh F.; Popowska M. *Front. Microbiol.* **2013**, 4. [Crossref]

[4] Blair J. M. A.; Webber M. A.; Baylay A. J.; Ogbolu D. O.; Piddock L. J. V. *Nat. Rev. Microbiol.* **2015,** *13*, 42. [Crossref]

[5] Hamid, A.; Mäser, P.; Mahmoud, A. B. *Molecules* **2024**, *29*, 635. [Crossref]

[6] Jayawardene, K. L. T. D.; Palombo, E. A.; Boag, P. R. *Biomolecules* **2021**, *4*, 1457. [Crossref]

[7] Guo, Y.; Hou, X.; Fang, H. *MRMC* **2021,** *30*, 1367. [Link]

[8] Atmaca, H.; İlhan, S.; Batır, M. B.; Pulat, C. C.; Güner, A. Bektaş H. *Chem.-Biol. Interact.* **2020,** *327*, 109163. [Crossref]

[9] Karan, R.; Agarwal, P.; Sinha, M.; Mahato, N. *ChemEngineering* **2021**, *5*, 73. [Crossref]

[10] Auti, P. S.; George, G.; Paul, A. T.; *RSC Adv.* **2020,** *10*, 41353. [Link]

[11] Lacey, E. *Parasitol. Today* **1990**, *6*, 112. [Crossref]

[12] Patel, H. M.; Shah, D. R. *Eur. J. Med. Chem.* **2015**, *97*, 664. [Crossref]

[13] Porter, T. N.; Li, Y.; Raushel, F. M. *Biochemistry* **2004,** *43*, 16285. [Crossref]

[14] Washabaugh, M. W.; Collins, K. D. *J. Biol. Chem.* **1986,** *261*, 5920. [Crossref]

[15] Kawatkar, S. P.; Keating, T. A.; Olivier, N. B.; Breen, J. N.; Green, O. M.; Guler, S. Y. *J. Med. Chem*. **2014,** *12*, 4584. [Crossref]

[16] Barakat, A.; Al-Majid, A. M.; Al-Qahtany, B. M.; Ali, M.; Teleb, M.; Al-Agamy, M. H. *Chem. Cent. J.* **2018,** *12*, 29. [Link]

[17] Morsy, M. A.; Ali, E. M.; Kandeel, M.; Venugopala, K. N.; Nair, A. B.; Greish, K. *Antibiotics* **2020,** *29*, 221. [Link]

[18] Vasantha Kumar, B. C. Synthesis characterization and applications of transition metal complexes with Schiff base ligands. 2018. (Thesis).

[19] Frisch, M. J.; Trucks, G. W.; Schlegel, H. B.; Scuseria, G. E.; Robb, M. A.; Cheeseman, J. R.; Fox, D. *J. Gaussian 09, Revision* D. 01, **2009**. [Link]

[20] Dennington, R.; Keith, T.; Millam, J. GaussView V. **2009**. *Semichem Inc. Shawnee Mission KS, GaussView, Version*, *5*(8). [Link]

[21] Maddili, S. K.; Li, Z. Z.; Kannekanti, V. K.; Bheemanaboina, R. R. Y.; Tuniki, B.; Tangadanchu, V. K. R. *Bioorg. Med. Chem. Lett.* **2018***, 28,* 2426. [Crossref]

[22] Thakkar, S. S.; Thakor, P.; Ray, A.; Doshi, H.; Thakkar, V. R. *Bioorg. Med. Chem.* **2017,** *25*, 5396. [Crossref]

[23] Mishra, V. R.; Ghanavatkar, C. W.; Mali, S. N.; Qureshi, S. I.; Chaudhari, H. K.; Sekar, N. *Comput. Biol. Chem.* **2019**, *78*, 330. [Crossref]

[24] Naaz, F.; Srivastava, R.; Singh, A.; Singh, N.; Verma, R.; Singh, V. K. *Bioorg. Med. Chem*. **2018,** *26*, 3414. [Crossref]

[25] Er, M.; Özer, A.; Direkel, Ş.; Karakurt, T.; Tahtaci, H. *J. Mol. Struct.* **2019,** *1194*, 284. [Crossref]

[26] Poirel L.; Madec J. Y.; Lupo A.; Schink, A. K.; Kieffer, N.; Nordmann P. *Microbiol. Spectr.* **2018**, *6*. [Crossref]

[27] Kelly, R. E.; Mally, M. I.; Evans, D. R. *J. Biol. Chem.* **1986,** *5*, 6073. PMID: 2871022

[28] Lee, M.; Maher, M. J.; Guss J. M. *Acta Crystallograph Sect. F Struct. Biol. Cryst. Commun.* **2007** *1*,154. [Crossref]

[29] Kotaka, M.; Dhaliwal, B.; Ren, J.; Nichols, C. E.; Angell, R.; Lockyer, M. *Protein Sci. Publ. Protein Soc.* **2006,** *5*, 774. [Crossref]

[30] Tian, W.; Chen, C.; Lei, X.; Zhao, J.; Liang J. *Nucleic Acids Res.* **2018**, *2*, W363. [Crossref]

[31] Arjunan, V.; Isaac, A. S. R.; Rani, T.; Mythili, C. V.; Mohan, S. *Spectrochim. Acta, Part A* **2011**, *78,* 1625. [Crossref]

[32] Parr, R. G.; Pearson, R. G. *J. Am. Chem. Soc.* **1983**, *105*, 7512. [Crossref]

[33] Kosar, B.; Albayrak, C. *Spectrochim. Acta, Part A* **2011**, *78*, 160. [Crossref]

[34] Fukui, K.; Koga, N.; Fujimoto, H. *J. Am. Chem. Soc.* **1981**, *103*, 196. [Crossref]

[35] Leboeuf, M.; Köster, A. M.; Jug, K.; Salahub, D. R. *J. Chem. Phys.* **1999**, *111,* 4893. [Crossref]

[36] Kamal, A.; Ramu, R.; Shaik, T. B. *Eur. J. Med. Chem.* **2013**, *64,* 180. [Crossref]

[37] Karthikeyan, M. S.; Prasad, D. J.; Poojary, B. *Eur. J. Med. Chem.* **2006**, *41*, 738. [Crossref]

How to cite this article

HR, G. K. M.; HD, R.; Avinash, K. O.; BC, V. K.; M, P. Harish, K. K. *Orbital: Electron. J. Chem*. **2025**, *17*, 464. DOI: http://dx.doi.org/10.17807/orbital.v17i5.23217